科学通报 2023 年 第 68 卷 第 32 期: 4401 ~ 4414
国家纳米科学中心成立20周年专辑 评 述
《中国科学》杂志社 SCIENCE CHINA PRESS

吡啶调控羧酸衍生物组装结构扫描隧道显微镜研究进展

张玉菲[1,2], 雷鹏[1,2], 孟婷[1,2], 王琛[1,2*], 曾庆涛[1,2*]

1. 国家纳米科学中心, 中国科学院纳米标准与检测重点实验室, 北京 100190;
2. 中国科学院大学材料科学与光电工程中心, 北京 100049
* 联系人, E-mail: wangch@nanoctr.cn; zengqd@nanoctr.cn

2023-05-28 收稿, 2023-08-28 修回, 2023-09-13 接受, 2023-09-14 网络版发表
国家自然科学基金(21972031, 22272039)、中国科学院战略性先导科技专项B类(XDB36000000)和吉林中科研伸科技有限公司资助

摘要 近几十年来, 有机功能小分子的超分子自组装引起了广泛的研究, 为在分子水平上构建功能纳米结构提供了理论基础. 扫描隧道显微镜的发明为探索二维表界面超分子自组装的结构和性质开辟了新的途径. 分子间氢键相互作用驱动的二维纳米结构已经受到广泛的关注. 由于氢键的方向性和饱和性以及固/液界面上溶剂共吸附等因素, 其中大部分体系研究的是同分子系统, 而双组分系统的可靠制备要求双组分体系的稳定性超过任一同分子体系的稳定性. 吡啶上存在的具有未共用电子对的N原子是良好的氢键受体. 目前研究表明, 在特定体系中, 羧基供体与吡啶受体能够直接基于氢键相互作用优先形成双组分体系. 本文综述了近期吡啶衍生物对羧酸自组装调控的研究进展, 聚焦于吡啶结构、羧酸结构及取代基团等因素对双组分体系的影响, 构建了丰富的双组分纳米结构, 为二维超分子自组装结构的调控提供了有效手段.

关键词 分子自组装, 羧酸分子, 吡啶调控, 扫描隧道显微镜

超分子组装是一个复杂的动态过程[1], 组装单元间通过氢键[2~4]、范德华力[5~7]、卤键[8~10]、金属/有机配位作用[11~13]等非共价相互作用最终形成热力学或动力学稳定的超分子组装结构[14]. 虽然单个非共价键的强度较共价键弱, 但体系内非共价力的总和允许超分子组装结构稳定存在且具有较好的可调节性[15~17]. 超分子组装是搭建分子层面上的功能化纳米结构和“自下而上”构筑纳米器件的有效手段[18~20]. 近年来, 关于二维固/液界面上超分子组装结构的研究取得了很多进展[21,22]. 二维界面作为分子在大范围内有规律组装的基底, 不仅使吸附在界面上的分子自由度降低, 还会引入分子-基底、溶剂-基底间相互作用, 进而对组装过程产生影响[23~25], 即基底可以诱导组装结构的多态性[26], 因此对制造结构复杂、功能新颖的二维纳米结构具有重要研究价值[27,28].

扫描隧道显微镜(scanning tunneling mcrscope, STM)是一种具有原子级分辨率、能够实时原位观察超分子自组装单层(self-assembled monolayer, SAM)的手段[29,30]. STM基于对探针和基底间距离敏感的隧道电流的响应, 得到界面吸附分子的电子云密度信息, 呈现为可视化的图像, 仅受限于分子的导电性, 适应于超高真空、宽温度范围等工作条件, 是进行表界面科学研究的重要手段[31~35].

氢键的方向性和饱和性等特点使羧酸分子的动态组装行为更加多样且可被预测[36~38], 有利于精准地控制超分子组装过程, 形成具有特定结构和功能的纳米分子网络[39~41]. 芳香羧酸羧基间的O–H···O双氢键已广泛用于二维超分子网络的构建[42,43]. 苯环上羧基数

引用格式: 张玉菲, 雷鹏, 孟婷, 等. 吡啶调控羧酸衍生物组装结构扫描隧道显微镜研究进展. 科学通报, 2023, 68: 4401–4414
Zhang Y F, Lei P, Meng T, et al. Progress in scanning tunneling microscopy research on the regulation of carboxylic acids and their derivatives assembled structures by pyridine (in Chinese). Chin Sci Bull, 2023, 68: 4401–4414, doi: 10.1360/TB-2023-0505

© 2023《中国科学》杂志社

量和位置的改变形成了多种组装形态，产生了线性带、锯齿形带、蜂窝状或玫瑰花结(花、超花)等组装结构. 此外, 研究还揭示了分子平面性、对称性等内部结构[44~46]和溶剂、浓度等外界条件[47~49]对芳香羧酸组装结构的影响，展现出氢键超分子组装网络良好的可协调性. 目前, 羧酸分子组装体已经被广泛应用于二维分子模板和三维有机框架的构建中[50~52].

氢键(X–H···Y)相互作用中供体、受体的竞争和替换使得氢键驱动的多组分超分子结构更加丰富[53~55]. 例如，可以通过向羧酸自组装结构中引入其他羧酸[56]、吡啶衍生物[57]等氢键供受体，打破O–H···O氢键形成的原始自组装，进而形成新的共组装结构. 譬如，具有相似对称性和官能团的1,3,5-苯三甲酸(TMA)和1,3,5-三(4-羧基苯基)苯(BTB)分子能够通过氢键共组装成6种非致密填充单层[58]，尺寸差异很大的C_3对称的BTB与苯并三噻吩-2,5,8-三羧酸(TBTTA)单元可以形成随机混合二维网络[59]. 吡啶分子是含有一个N原子的六元杂环，N原子和羧基间可以形成O–H···N氢键，部分或全部取代羧基间原有的O–H···O氢键[60,61]，使吡啶插入或在羧酸分子间建起“桥梁”[62]，从而形成更丰富且稳定的双组分纳米结构[63]. 本文主要综述了近期吡啶衍生物对羧酸及其衍生物组装结构的调控进展，展示了吡啶衍生物对扩展双组分纳米超分子结构库的重要作用.

1 吡啶衍生物对芳香羧酸分子自组装的调控

一般而言，羧基对称分布的刚性平面芳香羧酸分子通常能够以高度可预测的方式组装成有序网络[64,65]. 对称的H_4BTY分子(分子结构式见图1)的4个羧基通过4对饱和的O–H···O氢键相互作用形成大范围的自组装网络，分子中所有苯环都平行于高定向热解石墨(highly oriented pyrolytic graphite, HOPG)基底, 分子间氢键和分子与基底间的π-π相互作用共同稳定了自组装(图2(a), (b)). DPE和PDE分子中两个吡啶基团通过碳碳双键连接，它们是N原子相对位置不同的同分异构体. 实验发现，DPE不能调控H_4BTY的自组装，然而PDE分子可以通过吡啶N原子和羧基的羟基间形成两个O–H···N氢键，插入到两个相邻的H_4BTY分子中，形成“酸-吡啶-酸”形式的共组装体(图2(c), (d)). 这可能是因为PDE分子N原子的相对位置使共组装结构更紧密，增强了体系的稳定性. 此外，PEBP-C4、PEBP-C6和PEBP-C8系列联吡啶衍生物的共轭主链相同，区别在于侧链的长度不同. 实验中PEBP-C4不能调控H_4BTY的自组装，而PEBP-C6和PEBP-C8则能够与H_4BTY进

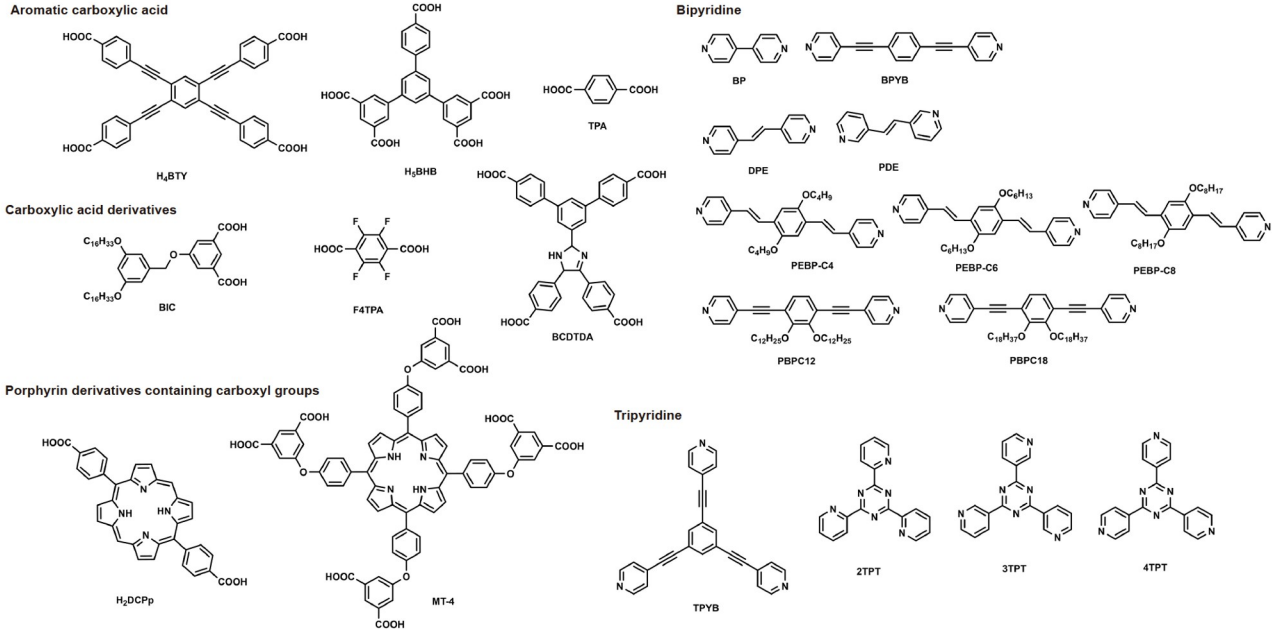


图 1 本文涉及的参与组装分子的化学结构式. 图中分子名称缩写对应的全称见表S1

Figure 1 Molecular chemical structures involved in assembly in this review. The full names corresponding to the abbreviations of molecular names in the figure are shown in Table S1

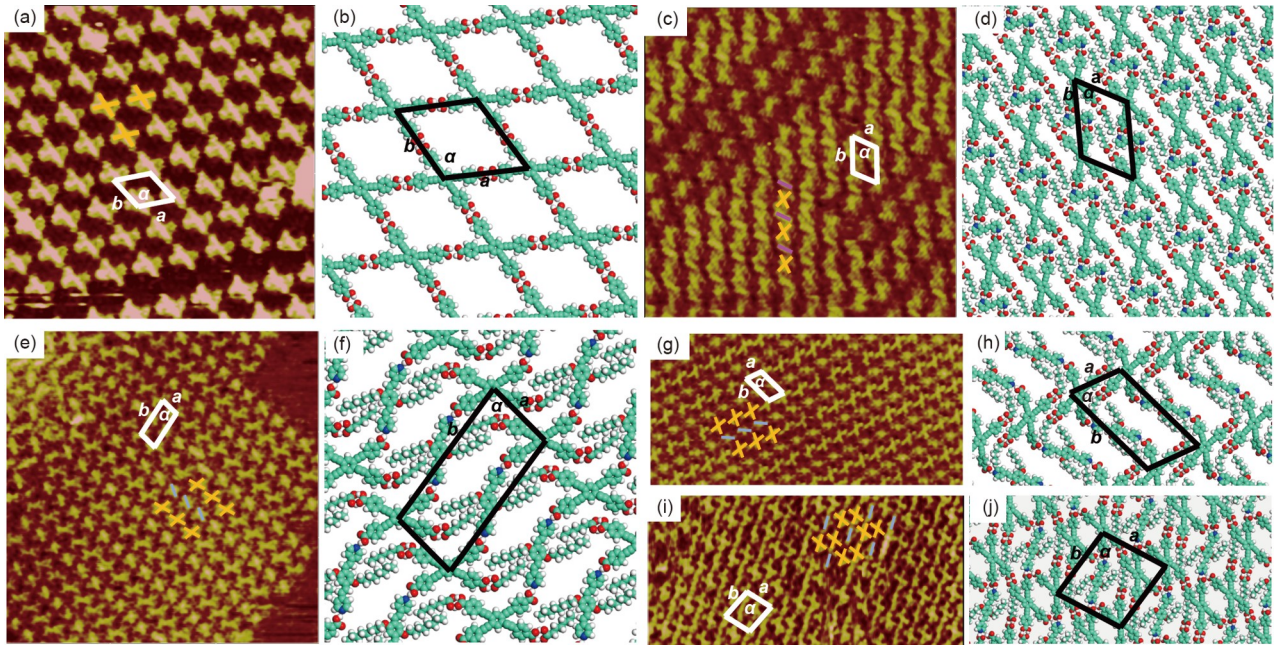


图 2 H_4BTY在庚酸(heptanoic acid, HA)/HOPG固/液界面上的自组装和与多种吡啶共组装的高分辨STM图像和分子模型[66], Copyright©2022, The Royal Society of Chemistry. (a), (b) H_4BTY自组装; (c), (d) H_4BTY-PDE共组装; (e), (f) H_4BTY-PEBP-C8共组装; (g), (h) H_4BTY-PEBP-C6-I共组装; (i), (j) H_4BTY-PEBP-C6-II共组装

Figure 2 High-resolution STM images and molecular models of H_4BTY self-assembly and co-assembly with various pyridines at the HA/HOPG solid/liquid interface[66], Copyright©2022, The Royal Society of Chemistry. (a), (b) H_4BTY self-assembly; (c), (d) H_4BTY-PDE co-assembly; (e), (f) H_4BTY-PEBP-C8 co-assembly; (g), (h) H_4BTY-PEBP-C6-I co-assembly; (i), (j) H_4BTY-PEBP-C6-II co-assembly

行共组装. PEBP-C8与H_4BTY规则排列为"酸-吡啶"交替的线性结构, 分子比例为1:1(图2(e), (f)). H_4BTY-PEBP-C6-I结构与其类似, 一个H_4BTY的两个羧基与两个吡啶分子的N原子形成O–H···N氢键, 另外两个羧基与庚酸(heptanoic acid, HA)溶剂形成O–H···O双氢键, 晶胞中分子比例为1:1(图2(g), (h)). 在结构II中, 一行中H_4BTY分子二聚体和PEBP-C6交叉排列, 两行间通过O–H···O和O–H···N氢键交错连接, 晶胞中分子比例为2:1(图2(i), (j)). 总之, PEBP-C4最短的丁烷氧基侧链之间因范德华相互作用较弱而不能与羧酸稳定地共组装, PEBP-C8最长的辛烷氧基侧链较大的空间位阻只能形成特定的共组装结构, PEBP-C6合适的己烷基侧链使其与H4BTY形成两种共组装结构. 这说明吡啶衍生物的空间特性(N原子位点和空间位阻)会限制羧酸和吡啶衍生物之间的相互作用[66].

由于对称的芳香羧酸分子更容易合成, 当前对于低对称性的芳香羧酸分子的自组装及调控的研究很少, 然而它们可能表现出更独特的组装行为[67,68]. 例如, H_5BHB分子含有5个羧基, 在石墨表面上可以近似为平面的, 但是其结构仅具有C_1对称性(分子结构见图1). 在其自组装过程中, 每两个H_5BHB分子先通过两对羧基之间的四重氢键紧密连接, 形成图3(b)中黄色虚线标记的C_2对称的二聚体, 之后两个取向的二聚体间彼此交错, 形成大规模的超分子自组装结构(图3(a)~(c)). 4,4′-联吡啶(BP)是一种D_2对称的线性联吡啶分子, 吡啶基团的N原子位于骨架两端. 3个H_5BHB二聚体和3个BP分子形成H_5BHB-BP共组装结构的最小重复构建块, 然后拼接成大范围的有序图案(图3(d), (e)). 在共组装结构中, H_5BHB二聚体与BP分子的比例为1:1(图3(f)). 这种独特的共组装结构的形成可能与H_5BHB二聚体的特殊氢键结合位点和BP分子的长度精确匹配有关. 在分子骨架更长的BPYB联吡啶衍生物与H_5BHB共组装时则有两种不同的结构(图3(g)). 在H_5BHB-BPYB-Stru1中, H_5BHB二聚体和BPYB分子的两端都与庚酸分子形成氢键, H_5BHB二聚体:BPYB:HA的分子比例为1:1:4(图3(h)). 在H_5BHB-BPYB-Stru2中, H_5BHB二聚体与BPYB分子一端的吡啶以O–H···N氢键连接, 而BPYB另一端的吡啶与HA连接, H_5BHB二聚体与BPYB分子和HA分子的比例为1:2:2(图3(i)). TPYB是一种D_{3h}对称三吡啶分子, 在与H_5BHB的共组装中, 每个H_5BHB二聚

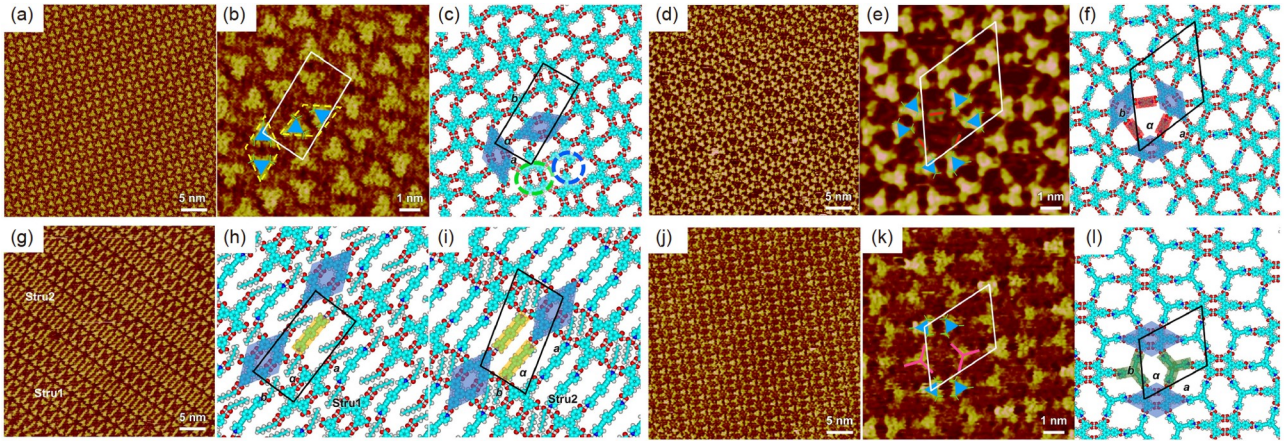


图 3 H_5BHB在庚酸/HOPG固/液界面上自组装和与多种吡啶共组装的高分辨的STM图像和分子模型[69], Copyright©2022, The Royal Society of Chemistry. (a)~(c) H_5BHB的自组装; (d)~(f) H_5BHB-BP的共组装; (g)~(i) H_5BHB-BPYB的两种共组装; (j)~(l) H_5BHB-TPYB的共组装

Figure 3 High resolution STM images and molecular models of H_5BHB self-assembly and co-assembly with various pyridines at the HA/HOPG solid/liquid interface[69], Copyright©2022, The Royal Society of Chemistry. (a)–(c) H_5BHB self-assembly; (d)–(f) H_5BHB-BP co-assembly; (g)–(i) two co-assembled structures of H_5BHB-BPYB; (j)–(l) H_5BHB-TPYB co-assembly

体被6个TPYB分子包围, 每个TPYB分子的3个吡啶基团通过3个O–H···N氢键与周围3个H_5BHB二聚体相连(图3(j)~(l)). 分子模型中清楚地标识出分子间相互作用, 且与STM图像十分吻合. 值得一提的是, 所有二元共组装结构都无法通过原位依次滴加两种分子制备, 而需要预先以合适的比例混合H_5BHB和吡啶溶液, 再将其混合溶液滴加在HOPG表面来制备, 说明二元共组装体系中存在动力学和热力学因素间的竞争, 而在预混合的二元系统中, 有序双组分共组装的形成是动力学优先事项[69].

2 吡啶衍生物对具有其他官能团取代的芳香羧酸衍生物自组装的调控

在含有较长烷基取代基的羧酸衍生物的自组装和调控中, 烷基链的导向作用以及分子与基底间相互作用的增强都会对界面吸附结构产生很大的影响[70]. 例如, BIC分子骨架的一侧为间苯二甲酸基团, 另一侧具有较长的烷基侧链, PBPC12和PBPC18吡啶衍生物具有相同的吡啶基团和乙炔骨架, 但具有不同的烷基取代基(分子结构式见图1). BIC能够与两种吡啶衍生物基于O–H···N氢键相互作用在固/液界面上形成新颖的共组装结构. BIC分子在1-辛酸(OA)/HOPG界面上形成线性自组装结构, OA溶剂插入在BIC分子之间(图4(a)). 在1-辛醇/HOPG界面上, 高浓度时($\geq 1 \times 10^{-5}$ mol L^{-1}), PBPC12与BIC共组装形成线性结构(图4(b), (c)), 而低浓度时($< 1 \times 10^{-5}$ mol L^{-1}), 它们则形成六聚体结构(图4(f)~(h)). BIC-PBPC12-high线性结构中每个蓝色的BIC分子的羧基和粉色的PBPC12分子的吡啶基团形成O–H···N氢键, 烷基链交叉排列在其中(图4(d)). 在这种共组装结构中, 吡啶类似于OA作为氢键受体插入BIC分子间(图4(e)), 烷基链的不同组织模式是单位晶胞不同的原因. 在BIC-PBPC12-low六聚体结构中, 每个六聚体由4个外部BIC分子和两个插入的PBPC12分子构建(图4(f)), 沿*a*方向上六聚体距离保持恒定(约为(6.8±0.2) nm), 而沿*b*方向上六聚体间距存在漂移(图4(g), (h)). 这也是由烷基链的组织模式引起的, 在*a*方向上BIC分子的十六烷基链交叉填充, 使得十六烷基链间的范德华相互作用最大化, 然而*b*方向上PBPC12的十二烷基链首尾相连, 对六聚体稳定的贡献很小(图4(i), (j)).

PBPC18与BIC共组装则只有一种规律的六聚体结构, 需要一段时间达到动态平衡状态(图4(k), (l)). 这也是由于更长的烷基链使得分子与底物的相互作用增加, 减缓了多组分自组装的动态过程. 六聚体结构与BIC-PBPC12-low的组织模式类似, 区别在于BIC-PBPC18六聚体能够形成稳定有序的阵列, 两种烷基链之间的角度约为60°(图4(m), (n)). 虽然A型和B型的六聚体在界面的平铺方向上不同, 但这两种类型的六聚体非常匹配, 在STM连续扫描过程中, 产生的随机平铺图案是稳定的. 引入柔性烷基侧链不仅能够增强组装体系的稳定性, 还可能作为柔性分子模板, 增加体系的容错率、多样性和可调性[71].

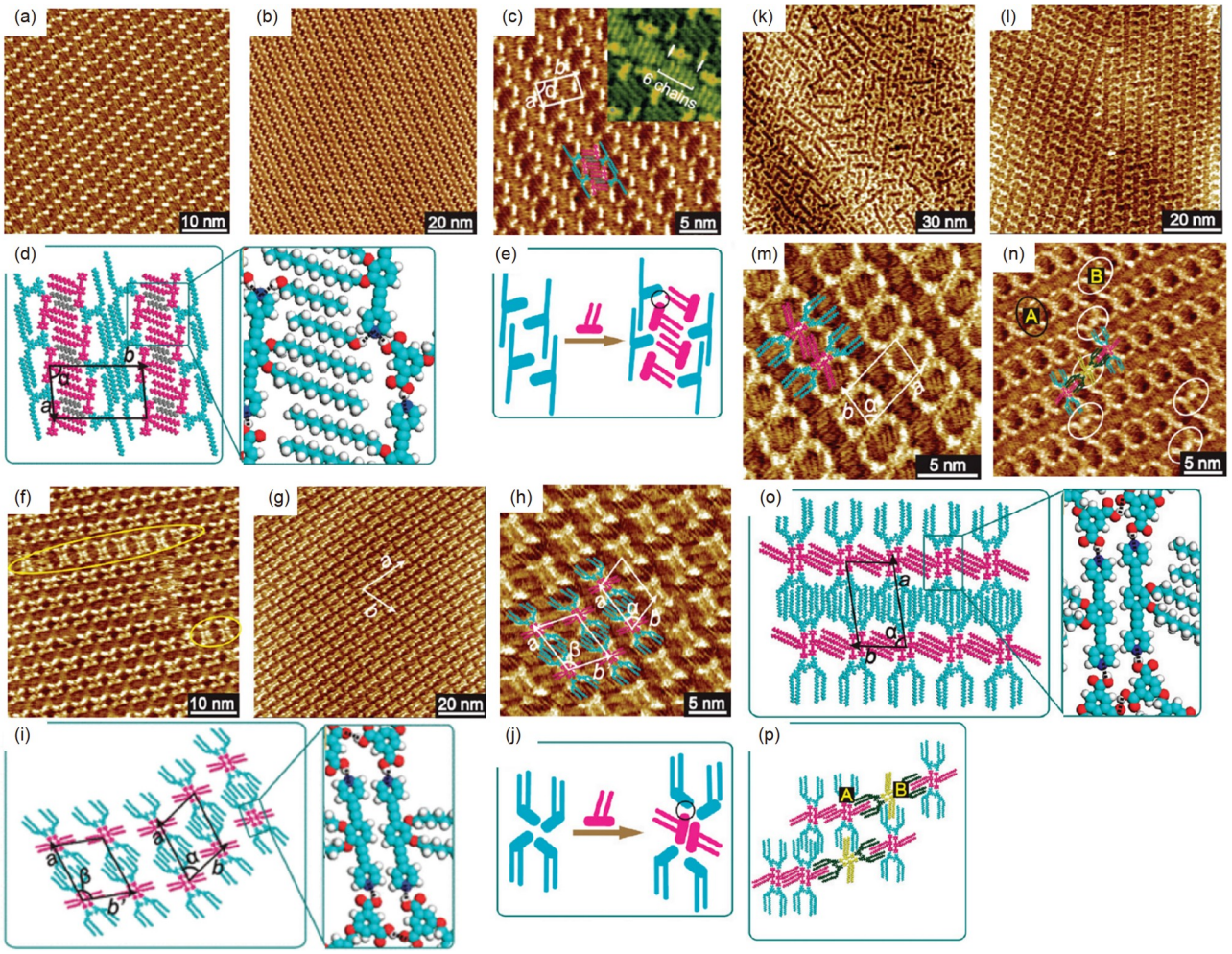


图 4 BIC在1-辛醇/HOPG固/液界面上的自组装和与多种吡啶共组装的大范围和高分辨的STM图像及分子模型[71], Copyright©2010, American Chemical Society. (a) BIC在1-辛酸/HOPG固/液界面上的自组装; (b), (c) BIC-PBPC12-high的线性共组装; (d), (e) PBPC12分子插入线性交错排列的BIC分子的模式; (f)~(h) BIC-PBPC12-low的六聚体共组装及在*b*轴方向的不同取向排列; (i), (j) PBPC12分子插入四角形排列的BIC分子的模式; (k)~(n) BIC-PBPC18的两种六聚体共组装; (o), (p) BIC-BPC18两种六聚体排列的分子模型

Figure 4 Large scale and high resolution STM images and molecular models of BIC self-assembly and co-assembly with various pyridines at the 1-octanol/HOPG solid/liquid interface[71], Copyright©2010, American Chemical Society. (a) BIC self-assembly on the 1-octanoic acid/HOPG interface; (b), (c) BIC-PBPC12-high linear co-assembly; (d), (e) the mode of PBPC12 inserting into linear staggered arranged BIC molecules; (f)–(h) BIC-PBPC12-low hexamer co-assembly and its different orientation in the *b*-axis direction; (i), (j) the mode of PBPC12 inserting into quadrangle arranged BIC molecules; (k)–(n) two hexamers co-assembly of BIC-PBPC18; (o), (p) molecular models of two BIC-PBPC18 hexamers co-assembly arrangement

对苯二甲酸TPA是研究氢键控制的自组装的典型分子, 容易自组装成可扩展的二维网络[72], 但对苯环的氟化阻止了F4TPA的自组装. 然而, 当与一系列吡啶衍生物氢键受体共组装时, F4TPA在形成双组分网络时反而优于TPA的构建块. 2TPT、3TPT和4TPT是3种三吡啶基三嗪异构体, N位点的相对位置不同(分子结构见图1). TPA分子只能与4TPT形成双组分网络(图5(a)), 每个4TPT分子的两个吡啶N原子通过O–H···N氢键与两侧相邻TPA分子相互作用, 次级的C–H···O=和C–H···N(吡啶基)相互作用也可能有助于稳定组装(图5(b))[73].

与TPA相比, 氟原子的吸电子能力可能使F4TPA与受体形成更强的O–H···N氢键. 此外, F4TPA可以产生额外的C–H···F相互作用, 也有助于稳定共组装结构. F4TPA-4TPT的双组装网络(图5(c), (d))的晶胞参数与TPA-4TPT的相同, 高分辨率STM图像中也显示两个体系的分子间相互作用是类似的, 反映了将H原子替换成F原子最小的立体影响. 在F4TPA-2TPT共组装中, 每个

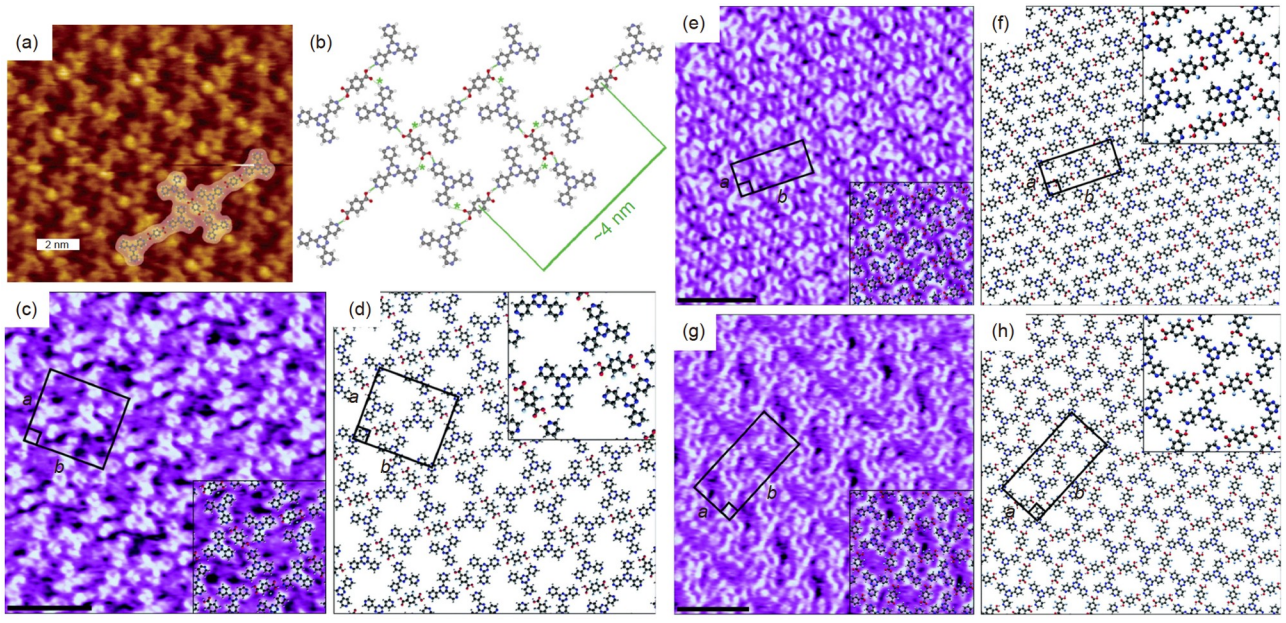


图 5 TPA和F4TPA在庚酸/HOPG固/液界面上与多种吡啶共组装的高分辨STM图像和分子模型. (a), (b) TPT-4TPT共组装[4], Copyright©2010, American Chemical Society; (c), (d) F4TPA-4TPT共组装; (e), (f) F4TPA-2TPT共组装; (g), (h) F4TPA-3TPT共组装[73], Copyright©2020, The Royal Society of Chemistry

Figure 5 High resolution STM images and molecular models of TPA and F4TPA co-assembly with various pyridines at the HA/HOPG solid/liquid interface. (a), (b) TPT-4TPT co-assembly[4], Copyright©2010, American Chemical Society; (c), (d) F4TPA-4TPT co-assembly; (e), (f) F4TPA-2TPT co-assembly; (g), (h) F4TPA-3TPT co-assembly[73], Copyright©2020, The Royal Society of Chemistry

2TPT分子的两个N原子参与了O–H···N相互作用, 额外的C–H···O=和C–H···F相互作用也有助于稳定结构 (图5(e), (f)). 3TPT作为氢键受体时的共组装结果与2TPT相似, 为了使最有利的O–H···N相互作用的数量最大化, 3TPTZ分子需要处于非三重对称构象(图5(g), (h)). 氟化可以显著改变羧酸分子的表面自组装行为, 虽然周边氟化会防止单分子自组装, 但它在构建双组分网络方面显示出明显的优势[4].

咪唑是一种五元杂环化合物, 具有两个N原子位点, 其中一个具有一对单独的电子, 是常见的氢键供体[74]. 含有咪唑基团的羧酸衍生物可能形成N–H···O氢键, 导致不同的组装模式[40], 对这种组装体系的研究尚且不多. BCDTDA自组装形成两种结构(图6(a)), 一个分子咪唑基团上的N–H和相邻分子羧基的羰基O原子(图6(b)中的蓝色圆圈)形成了一对N–H···O氢键, 先形成二聚体构建块. 二聚体的剩余羧基则与周围的二聚体形成O–H···O氢键(图6(b)中的红色圆圈), 最终自组装形成规则的井字网格结构. 二聚体还能够组装为Kagomé结构, 6个二聚体连接成六元环, 暴露于六边形空腔的羧基与HA溶剂共组装, 周围的3个二聚体形成一个小的三角形空腔(图6(c)). 含氮杂环取代的羧酸衍生物的自组装受到分子结构和N位点的影响.

吡啶分子对以二聚体为单元的BCDTDA自组装网络有两种不同的调控模式. 首先, BP分子不能破坏其二聚体结构, 每行中相邻的二聚体由两个平行的BP分子桥接起来(图6(d), (e)). 然而, 在PEBP-C4和PEBP-C8对BCDTDA的调控中, N–H···O氢键二聚体结构被破坏. PEBP-C4与BCDTDA只有一种共组装结构(图6(f)), 两个BCDTDA分子通过羧基间的一对O–H···O氢键形成二聚体(图6(g)中红色圆圈), PEBP-C4分子通过O–H···N(吡啶)氢键(图6(g)中蓝色和黄色圆圈)与相邻BCDTDA分子连接, 其余暴露的所有羧基和吡啶基团都与HA溶剂共吸附. 尽管PEBP-C8分子只是烷基侧链比PEBP-C4略长, 但其与BCDTDA分子却有3种双组分共组装结构, 3种结构的面积比约为3∶2∶1(图6(h), (j), (l)), 3种结构中酸和吡啶的分子比例分别为2∶3(图6(i))、1∶2(图6(k))和1∶1(图6(m)). 不同的联吡啶分子对二聚体表现出不同的调节作用, 可能会破坏或保留二聚体的形成, 最终是为了达到热力学稳定, 这也为羧酸二聚体的调控实验方案提供了新的途径[75].

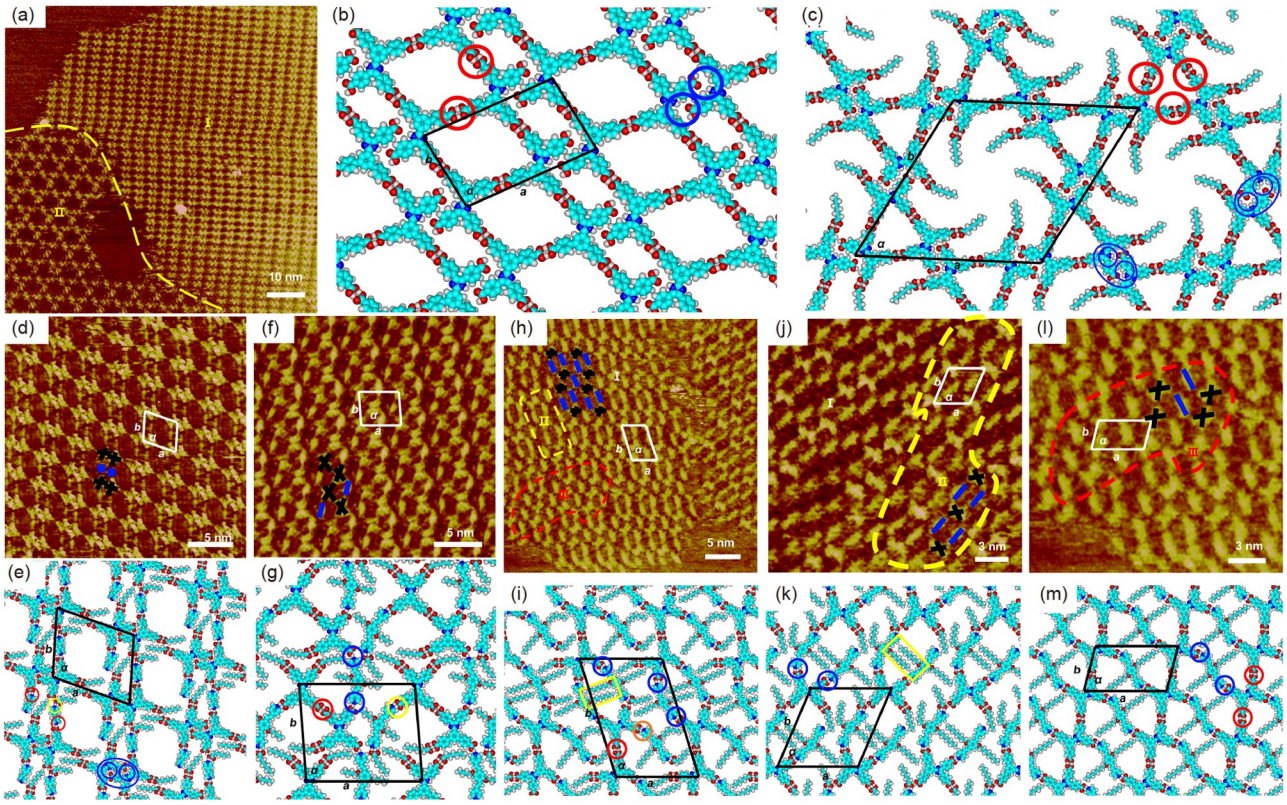


图 6 BCDTDA在庚酸/HOPG固/液界面上的自组装和与多种联吡啶共组装的大范围和高分辨STM图像和分子模型[75], Copyright©2022, Elsevier. (a)~(c) BCDTDA的两种自组装; (d), (e) BCDTDA-BP的共组装; (f), (g) BCDTDA-PEBP-C4的共组装; (h), (i) BCDTDA-PEBP-C8-I共组装; (j), (k) BCDTDA-PEBP-C8-II共组装; (l), (m) BCDTDA-PEBP-C8-III共组装

Figure 6 Large scale, high resolution STM images and molecular models of BCDTDA self-assembly and co-assembly with various bipyridines at the HA/HOPG solid/liquid interface[75], Copyright©2022, Elsevier. (a)–(c) Two kinds of BCDTDA self-assemblies; (d), (e) BCDTDA-BP co-assembly; (f), (g) BCDTDA-PEBP-C4 co-assembly; (h), (i) BCDTDA-PEBP-C8-I co-assembly; (j), (k) BCDTDA-PEBP-C8-II co-assembly; (l), (m) BCDTDA-PEBP-C8-III co-assembly

3 含羧基的卟啉衍生物的自组装及吡啶调控

卟啉及其衍生物以其优异的光学和电学性能而闻名[76], 通过二维表面上的氢键研究卟啉组装已成为当下的研究热点, 因为带有羧基官能团的卟啉衍生物通过氢键相互作用形成超分子纳米结构, 有助于光电材料制备的优化[77]. STM图像中呈菱形的H_2DCPp分子自组装形成紧密的线性排列(图7(a)), 每个H_2DCPp分子的末端羧基与另外两个分子形成一对“头对头”的O–H···O氢键(图7(b)红色圆圈).

BPYB分子中心苯环的对位被炔键和吡啶基组成的取代基取代. 向H_2DCPp自组装结构中引入BPYB分子后, BPYB分子插入两个H_2DCPp分子之间, 吡啶的N原子和羟基–OH形成一个O–H···N氢键, 相邻苯环上的H原子和羰基O原子形成一个C–H···O=氢键(图7(c), (d)). 两种氢键共同稳定共组装结构, 同时由于空间位阻, BPYB分子中的碳碳单键有一定程度的弯曲.

BP分子与H2DCPp分子共组装时同时出现两种共组装结构(图7(e), (g)). 在H_2DCPp-BP-I结构中, BP分子没有破坏H_2DCPp分子间O–H···O氢键, BP分子的一个吡啶N原子和卟啉环上的H原子相距约0.23 nm, 形成C–H···N氢键, 另一个吡啶N原子与苯甲酸取代基中苯环上的H原子间的距离约为0.27 nm, 形成C–H···N氢键. BP分子和H_2DCPp分子的卟啉环间的“边-面”π-π相互作用进一步增强了体系中分子间作用力的多样性, 有助于共组装结构的稳定性(图7(f)). H_2DCPp-BP-II结构与之相似, 但BP分子转动了约90°, 几乎垂直于H_2DCPp分子, 吡啶的两个N原子分别与苯甲酸上苯环的H原子形成两种C–H···N氢键(图7(h)中蓝色和紫色圆圈), 间距分别约为0.22和0.21 nm. 此外, BP分子的吡

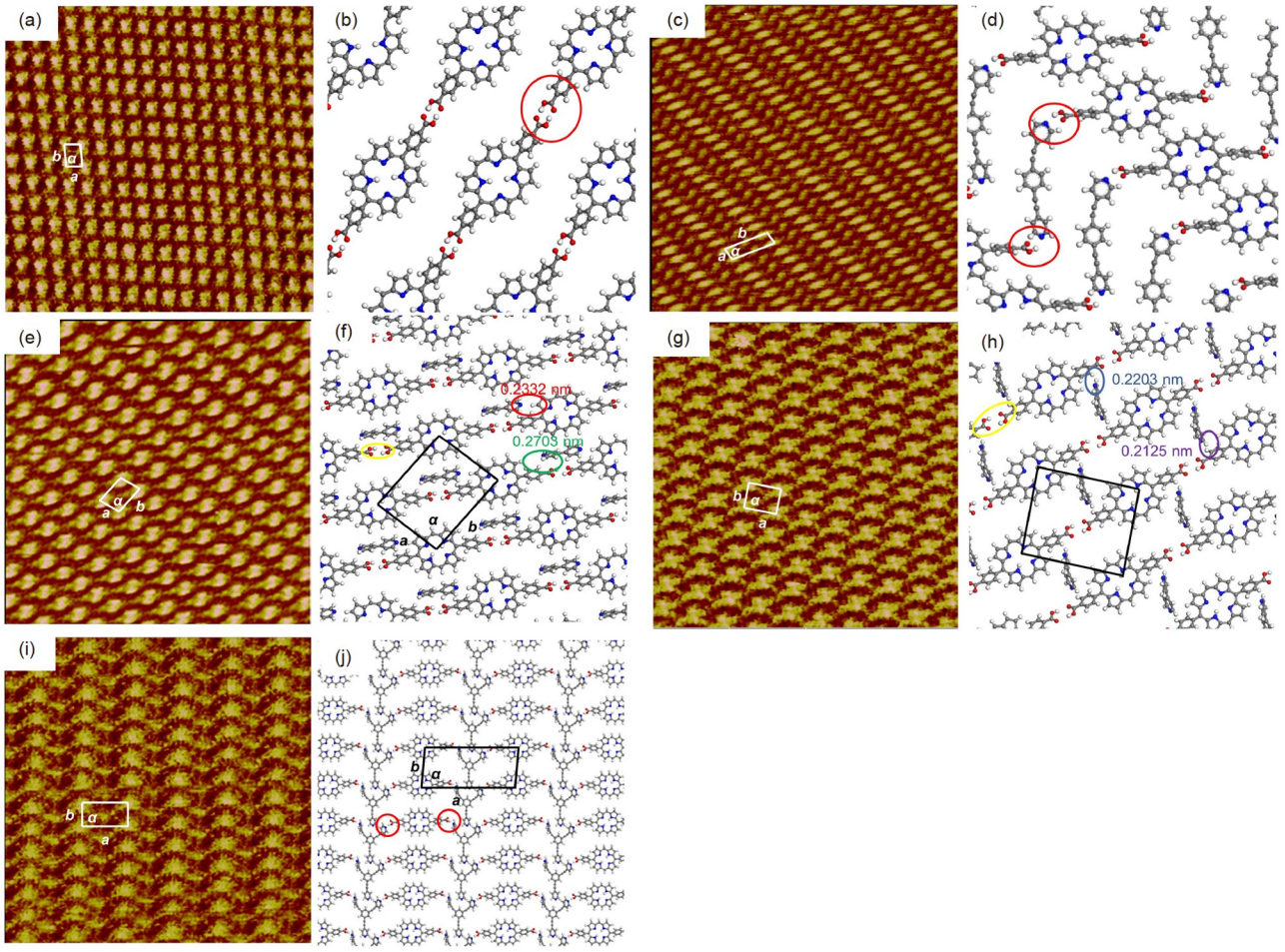


图 7 H_2DCPp在庚酸/HOPG固/液界面上的自组装和与多种吡啶共组装的高分辨STM图像和分子模型[78], Copyright©2021, American Chemical Society. (a), (b) H_2DCPp的自组装; (c), (d) H_2DCPp-BPYB的共组装; (e), (f) H_2DCPp-BP-I的共组装; (g), (h) H_2DCPp-BP-II的共组装; (i), (j) H_2DCPp-TPYB的共组装

Figure 7 High resolution STM images and molecular models of H_2DCPp self-assembly and co-assembly with various bipyridines at the HA/HOPG solid/liquid interface[78], Copyright©2021, American Chemical Society. (a), (b) H_2DCPp self-assembly; (c), (d) H_2DCPp-BPYB co-assembly; (e), (f) H_2DCPp-BP-I co-assembly; (g), (h) H_2DCPp-BP-II co-assembly; (i), (j) H_2DCPp-TPYB co-assembly

啶和H_2DCPp的苯环间偏移的“面对面”堆叠也可以增强共组装的稳定性(图7(h)). TPYB分子是以苯环为中心的C_3对称吡啶衍生物, 成功地调控了H_2DCPp自组装结构, TPYB分子以O–H···N氢键连接在两个H_2DCPp分子之间, 形成手牵手的有序共组装结构(图7(i), (j))[78].

MT-4分子中心为卟啉核心, meto位为4个取代的苯基, 其中一个是间苯二甲酸基团(分子结构见图1). 不同溶剂中MT-4的自组装结构不同. 以辛基苯(phenyloctane, PO)为溶剂时, MT-4分子形成高度有序的线性排列的自组装单层. 由于卟啉核心较高的电子云密度, 空心的X形亮点代表MT-4分子的核心, 亮度较暗的直线对应其平行排列的溶剂和MT-4分子的烷基侧链(图8(a), (b))[79]. 外围苯环与卟啉中心平面约成70°角并采用“边对面”构型以最小化空间位阻. 在HA溶剂中, HA的羧基与MT-4分子形成氢键, 形成了四方的自组装结构(图8(c), (d)).

在MT-4-DPE共组装中, 短亮棒代表的DPE分子横跨在MT-4分子行之间(图8(e)). 每个DPE的两个吡啶基团可以与两个相邻MT-4分子的苯环或卟啉核(平均长度0.352 nm)构建一对C–H···N氢键, 分子的苯环在HOPG表面上均采用“边对面”构型(图8(f)). PBEP-C8的引入引起MT-4自组装结构发生类似的改变, PEBP-C8分子连接起MT-4分子行, 共组装成二维有序结构, 两

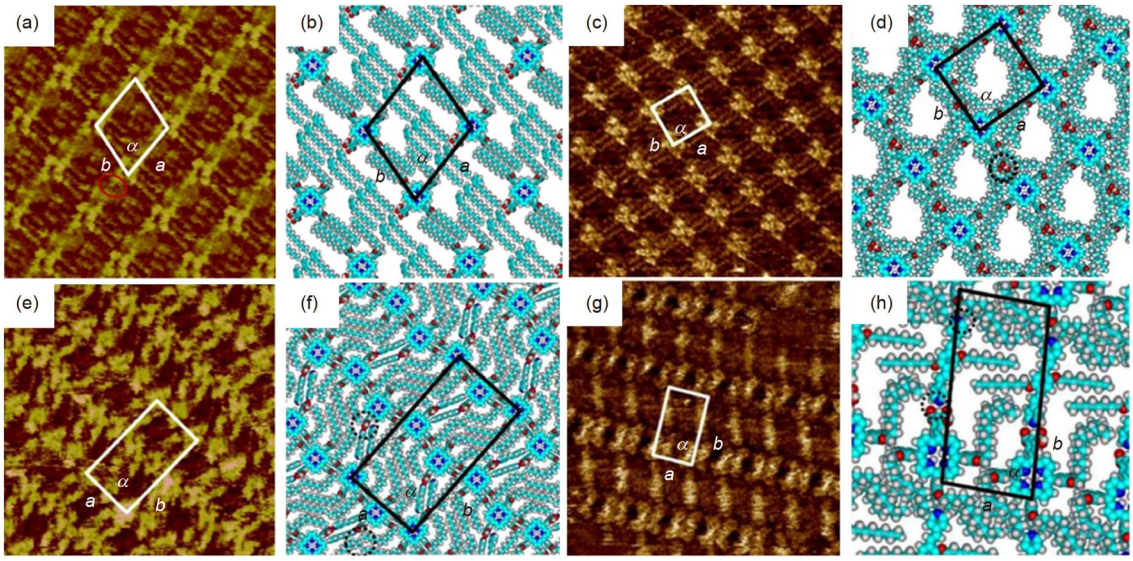


图 8 MT-4在固/液界面上的自组装和与多种吡啶共组装的高分辨STM图像和分子模型[79], Copyright©2020, American Chemical Society. (a), (b) MT-4在辛基苯(Phenyloctane, PO)/HOPG界面上的自组装; (c), (d) MT-4在庚酸/HOPG界面上的自组装; (e), (f) MT-4-DPE在辛基苯/HOPG界面上的共组装; (g), (h) MT-4-PEBP-C8在辛基苯/HOPG界面上的共组装

Figure 8 High resolution STM images and molecular models of MT-4 self-assembly and co-assembly with various bipyridines at the solid/liquid interface[79], Copyright©2020, American Chemical Society. (a), (b) MT-4 self-assembly at PO/HOPG interface; (c), (d) MT-4 self-assembly at HA/HOPG interface; (e), (f) MT-4-DPE co-assembly at PO/HOPG interface; (g), (h) MT-4-PEBP-C8 co-assembly at PO/HOPG interface

个吡啶N通过一对C–H···N氢键(平均长度0.349 nm)与两个相邻MT-4分子的苯环相互作用(图8(g), (h)). 区别在于由于空间位阻效应, MT-4和PEBP-C8分子共组装结构更松散, 所有PEBP-C8的烷基侧链能够充分延伸, 而MT-4分子的取代烷基则不能全部拉伸. DPE和PEBP-C8分子不同化学结构导致了HA/HOPG界面上不同共组装结构的出现[79].

4 总结与展望

STM能够清楚直观地探究界面分子吸附层的结构, 已经发展成为研究固/液界面自组装单层的高效手段. 对超分子自组装机理的深入认识有助于拓宽功能纳米结构的合成路径. 因此, 近些年来利用STM技术探究二维界面超分子结构的研究逐渐兴起. 氢键的方向性和饱和性等特点使其被广泛地应用在三维晶体中和二维界面上的功能体系构建中. 本综述主要总结了氢键驱动的超分子自组装网络的STM研究进展, 展现了由芳香羧酸及其衍生物的分子结构带来的多样的单组分自组装结构, 总结了吡啶衍生物具备对羧酸自组装良好的调控能力, 能够形成结构新颖的双组分共组装结构, 并且对比了不同的调控模式, 有助于进一步深入理解以氢键为驱动力的组装结构的形成和调控. 当前的研究表明, 在特定体系中, 羧基和吡啶分别作为氢键的供体和受体, 可以引起单元体系转变为基于不同氢键的二元体系. 本文重点讨论了吡啶和羧酸的官能团、取代基的数量和位置、分子结构等因素对二元体系的影响. 首先, 高对称性的芳香羧酸的自组装及其与吡啶衍生物的共组装行为与低对称性的芳香羧酸有显著不同; 柔性烷基侧链具有结构定向能力, 可以作为分子模板容纳不同尺寸和形状的吡啶乙炔基衍生物. 其次, 羧酸的氟化可以阻止其自组装, 但展现出与不同吡啶构建二元网络的优势; 引入不同N杂环的羧酸衍生物表现出特定的共组装模式. 这些多样的共组装行为的产生可能是由氢键供体和受体的不同强度引起的. 此外, 羧基还能够通过氢键帮助卟啉衍生物在表面上形成有序排列, 并且使其可以被不同种类的吡啶调节. 总之, 当前研究者们已经构建了丰富多元的表面纳米结构, 拓展了多组分超分子组装结构的制备和调控手段.

然而, 该领域的发展有望进一步深入. 首先, 我们还可以继续拓宽表面纳米结构的基本构建块. 比如, 对于三联吡啶衍生物和羧酸共组装行为的研究还不够充分, 目前的研究主要使用较小的三吡啶, 还可以继续增大骨架的刚性或者调整N位点的相对位置等, 可能会出现更丰富的组装结构. 我们还可以不断增加吡啶基团

的数量, 观察比较两种类型氢键数量的比例, 进一步加深对吡啶和羧酸两种组分形成的共组装结构的理解. 其次, 目前对于表面自组装的过程和机理的理解还不够, 我们还不能够准确地预测出组装结构. 我们还可以结合更多的表面检测手段, 对二维自组装的机理进行更深入的探究. 总之, 该领域的研究正在逐渐丰富, 对表面纳米结构的构建有一定指导意义, 我们还期望其能够在功能化等应用方面得到进一步的发展.

参考文献

1 Lehn J M. Supramolecular chemistry: From molecular information towards self-organization and complex matter. Rep Prog Phys, 2004, 67: 249–265
2 Slater A G, Perdigão L M A, Beton P H, et al. Surface-based supramolecular chemistry using hydrogen bonds. Acc Chem Res, 2014, 47: 3417–3427
3 Argent S P, Golden E, Ring D J, et al. Two-dimensional networks of thiocyanuric acid and imine bases assisted by weak hydrogen bonds. Cryst Growth Des, 2019, 19: 5945–5954
4 Pinfold H, Greenland C, Pattison G, et al. Fluorinated carboxylic acids as powerful building blocks for the formation of bimolecular monolayers. Chem Commun, 2020, 56: 125–128
5 Wu P, Zeng Q, Xu S, et al. Molecular superlattices induced by alkyl substitutions in self-assembled triphenylene monolayers. ChemPhysChem, 2001, 2: 750–754
6 Kalashnyk N, Gouesmel A, Kim E, et al. Functional hybrid multilayered van der Waals heterostructures from graphene and self-assembled supramolecular 2D crystals. 2D Mater, 2019, 6: 045016
7 Zhang X, Ding H, Chen X, et al. Complex supramolecular tessellations with on-surface self-synthesized C_{60} tiles through van der Waals interaction. Nanoscale, 2022, 14: 1333–1339
8 Metrangolo P, Meyer F, Pilati T, et al. Halogen bonding in supramolecular chemistry. Angew Chem Int Ed, 2008, 47: 6114–6127
9 Lawrence J, Sosso G C, Đorđević L, et al. Combining high-resolution scanning tunnelling microscopy and first-principles simulations to identify halogen bonding. Nat Commun, 2020, 11: 2103–2120
10 Xiao Y, Cai F, Peng X, et al. Aza-BODIPY molecular assembly at the liquid-solid interface driven by Br···F BF interactions. Chin Chem Lett, 2021, 32: 3566–3569
11 Li S S, Northrop B H, Yuan Q H, et al. Surface confined metallosupramolecular architectures: Formation and scanning tunneling microscopy characterization. Acc Chem Res, 2009, 42: 249–259
12 Zhang X, Shen Y, Wang S, et al. One plus two: Supramolecular coordination in a nano-reactor on surface. Sci Rep, 2012, 2: 742
13 Geng Y F, Wu S L, Xu J, et al. Formation of heterocaryotic and homonuclear bridged-dimeric complexes on surface. Chin Chem Lett, 2016, 27: 602–606
14 Mazur U, Hipps K W. Kinetic and thermodynamic processes of organic species at the solution-solid interface: The view through an STM. Chem Commun, 2015, 51: 4737–4749
15 Wei Y, Tong W, Wise C, et al. Dipolar control of monolayer morphology: Spontaneous SAM patterning. J Am Chem Soc, 2006, 128: 13362–13363
16 Guo Z, Tahara K, Inukai K, et al. Effect of multiple interactions on face-on vs. edge-on configurations of butadiyne-bridged octadehydrodibenzo [12]annulene derivatives at the liquid/graphite interface. J Phys Chem C, 2015, 119: 15977–15981
17 Maeda M, Nakayama R, De Feyter S, et al. Hierarchical two-dimensional molecular assembly through dynamic combination of conformational states at the liquid/solid interface. Chem Sci, 2020, 11: 9254–9261
18 Grimme S, Antony J, Ehrlich S, et al. A consistent and accurate *ab initio* parametrization of density functional dispersion correction (DFT-D) for the 94 elements H–Pu. J Chem Phys, 2010, 132: 154104
19 Liu J, Chen T, Deng X, et al. Chiral hierarchical molecular nanostructures on two-dimensional surface by controllable trinary self-assembly. J Am Chem Soc, 2011, 133: 21010–21015
20 Würthner F. Dipole-dipole interaction driven self-assembly of merocyanine dyes: From dimers to nanoscale objects and supramolecular materials. Acc Chem Res, 2016, 49: 868–876
21 Mali K S, Pearce N, De Feyter S, et al. Frontiers of supramolecular chemistry at solid surfaces. Chem Soc Rev, 2017, 46: 2520–2542
22 Goronzy D P, Ebrahimi M, Rosei F, et al. Supramolecular assemblies on surfaces: Nanopatterning, functionality, and reactivity. ACS Nano, 2018, 12: 7445–7481
23 Huang H, Wong S L, Chen W, et al. LT-STM studies on substrate-dependent self-assembly of small organic molecules. J Phys D-Appl Phys, 2011, 44: 464005

24 Niu T, Zhang J, Chen W. Molecular ordering and dipole alignment of vanadyl phthalocyanine monolayer on metals: The effects of interfacial interactions. J Phys Chem C, 2014, 118: 4151–4159

25 Tian G, Shen Y, He B, et al. Effects of monolayer Bi on the self-assembly of DBBA on Au(111). Surf Sci, 2017, 665: 89–95

26 Badami-Behjat A, Deimel P S, Allegretti F, et al. Versatile role of molecule-surface interactions for monolayer self-assembly at liquid-solid interfaces: Substrate-induced polymorphism, thermodynamic stability, and new polymorphs. Chem Mater, 2022, 34: 8876–8884

27 Ciesielski A, Palma C A, Bonini M, et al. Towards supramolecular engineering of functional nanomaterials: Pre-programming multi-component 2D self-assembly at solid-liquid interfaces. Adv Mater, 2010, 22: 3506–3520

28 Zhang J L, Ye X, Gu C, et al. Non-covalent interaction controlled 2D organic semiconductor films: Molecular self-assembly, electronic and optical properties, and electronic devices. Surf Sci Rep, 2020, 75: 100481

29 Cyr D M, Venkataraman B, Flynn G W. STM investigations of organic molecules physisorbed at the liquid-solid interface. Chem Mater, 1996, 8: 1600–1615

30 Yu L, Yang Y, Wang C, Peptide self-assembly and its modulation: Imaging on the nanoscale. In: Perrett S, Buell A K, Knowles T P J, eds. Biological and Bio-Inspired Nanomaterials. Singapore: Springer Nature Singapore Pte Ltd., 2019. 35–60

31 Dai H L, Geng Y F, Zeng Q D, et al. Photo-regulation of 2D supramolecular self-assembly: On-surface photochemistry studied by STM. Chin Chem Lett, 2017, 28: 729–737

32 Cui D, MacLeod J M, Rosei F. Probing functional self-assembled molecular architectures with solution/solid scanning tunnelling microscopy. Chem Commun, 2018, 54: 10527–10539

33 Zhang Y C, Lee D Y, Hipps K W. Characterizing the CH_3SSCH_3–Au(111) system from single molecules to full surface coverage: A scanning tunneling microscopy study. J Phys Chem C, 2021, 125: 21988–21996

34 Lei P, Li Q, Meng T, et al. Diverse self-assembly structures of a macrocycle revealed with STM by adjusting the solution concentration. Chem — An Asian J, 2022, 17: e202101246

35 Feng Y C, Wang X, Yi Z Y, et al. *In-situ* ECSTM investigation of H_2O_2 production in cobalt—Porphyrin-catalyzed oxygen reduction reaction. Sci China Chem, 2022, 66: 273–278

36 Li J, Luo W, Zhang S, et al. The effect of multiple pairs of meta-dicarboxyl groups on molecular self-assembly and the selective adsorption of coronene by hydrogen bonding and van der Waals forces. Nano Res, 2021, 15: 1691–1697

37 MacLeod J M, Ben Chaouch Z, Perepichka D F, et al. Two-dimensional self-assembly of a symmetry-reduced tricarboxylic acid. Langmuir, 2013, 29: 7318–7324

38 Griessl S, Lackinger M, Edelwirth M, et al. Self-assembled two-dimensional molecular host-guest architectures from trimesic acid. Single Mol, 2002, 3: 25–31

39 Cheng L, Tu B, Xiao X, et al. On-surface crystallization behaviors of H-bond donor-acceptor complexes at liquid/solid interfaces. Langmuir, 2019, 35: 8935–8942

40 Korolkov V V, Baldoni M, Watanabe K, et al. Supramolecular heterostructures formed by sequential epitaxial deposition of two-dimensional hydrogen-bonded arrays. Nat Chem, 2017, 9: 1191–1197

41 Peng X, Xiao Y, Mu B, et al. Programmable binary crystallization behaviors assisted by hydrogen bond on HOPG surface. Appl Surf Sci, 2021, 565: 150529

42 Leasor C, Chen K H, Closson T, et al. Revealing the structural complex of adsorption and assembly of benzoic acids at electrode-electrolyte interfaces using electrochemical scanning tunneling microscopy. J Phys Chem C, 2019, 123: 13600–13609

43 Li J, Tu B, Li X, et al. Self-assembled flower structures formed by C_3-symmetric aromatic carboxylic acids with *meta*-carboxyl groups. Chem Commun, 2019, 55: 11599–11602

44 Reynaerts R, Minoia A, Gali S M, et al. Coplanar versus noncoplanar carboxyl groups: The influence of sterically enforced noncoplanarity on the 2D mixing behavior of benzene tricarboxylic acids. J Phys Chem C, 2020, 124: 24874–24882

45 Wang J, Wang L M, Lu C, et al. Formation of multicomponent 2D assemblies of C_{2v}-symmetric terphenyl tetracarboxylic acid at the solid/liquid interface: Recognition, selection, and transformation. RSC Adv, 2019, 9: 11659–11663

46 Florio G M, Stiso K A, Campanelli J S. Surface patterning of benzenecarboxylic acids: Influence of structure, solvent, and concentration on molecular self-assembly. J Phys Chem C, 2012, 116: 18160–18174

47 Ochs O, Hocke M, Spitzer S, et al. Origin of solvent-induced polymorphism in self-assembly of trimesic acid monolayers at solid-liquid interfaces. Chem Mater, 2020, 32: 5057–5065

48 MacLeod J M, Lipton-Duffin J A, Cui D, et al. Substrate effects in the supramolecular assembly of 1,3,5-benzene tricarboxylic acid on graphite and graphene. Langmuir, 2015, 31: 7016–7024

49 Gutzler R, Sirtl T, Dienstmaier J F, et al. Reversible phase transitions in self-assembled monolayers at the liquid-solid interface: Temperature-controlled opening and closing of nanopores. J Am Chem Soc, 2010, 132: 5084–5090

50 Wang B, Lin R B, Zhang Z, et al. Hydrogen-bonded organic frameworks as a tunable platform for functional materials. J Am Chem Soc, 2020, 142: 14399–14416

51 Song X, Wang Y, Wang C, et al. Design rules of hydrogen-bonded organic frameworks with high chemical and thermal stabilities. J Am Chem Soc, 2022, 144: 10663–10687

52 Frederick E, Cojal González J D, Rabe J P, et al. Two-dimensional versus three-dimensional self-assembly of a series of 5-alkoxyisophthalic acids. Langmuir, 2018, 34: 10739–10747

53 Qian Y, Gu Y, Feng J, et al. Role of synergistic C–H···N and C–H···O H-bonding interactions in self-assemblies of a phthalocyanine derivative and several pyridine derivatives. J Phys Chem C, 2018, 122: 24158–24163

54 Rogers R D, Sharma C V K, Whitcomb D R. Molecular tweezers and pentameric aggregates: Convergent hydrogen-bonded self-assembly of 2∶1 and 2∶3 cocrystals of phthalazine: Phthalic acid. Cryst Eng, 1998, 1: 255–262

55 Velpula G, Li M, Hu Y, et al. Hydrogen-bonded donor-acceptor arrays at the solution-graphite interface. Chem Eur J, 2018, 24: 12071–12077

56 Li J, Zu X, Qian Y, et al. Advances in self-assembly and regulation of aromatic carboxylic acid derivatives at HOPG interface. Chin Chem Lett, 2020, 31: 10–18

57 Li X, Zhang S, Li J, et al. Advances in the regulation of bipyridine derivatives on two-dimensional (2D) supramolecular nanostructures. New J Chem, 2019, 43: 13315–13325

58 Kampschulte L, Werblowsky T L, Kishore R S K, et al. Thermodynamical equilibrium of binary supramolecular networks at the liquid-solid interface. J Am Chem Soc, 2008, 130: 8502–8507

59 MacLeod J M, Lipton-Duffin J, Fu C, et al. A 2D substitutional solid solution through hydrogen bonding of molecular building blocks. ACS Nano, 2017, 11: 8901–8909

60 Steiner T. The hydrogen bond in the solid state. Angew Chem Int Ed, 2002, 41: 48–76

61 Peng X, Cheng L, Zhu X, et al. Erratum to: Pyridine-induced interfacial structural transformation of tetraphenylethylene derivatives investigated by scanning tunneling microscopy. Nano Res, 2018, 11: 6110

62 Zhang X, Wang S, Shen Y, et al. Two-dimensional networks of an azobenzene derivative: Bi-pyridine mediation and photo regulation. Nanoscale, 2012, 4: 5039

63 Li M, Yang Y L, Zhao K Q, et al. Bipyridine-mediated assembling characteristics of aromatic acid derivatives. J Phys Chem C, 2008, 112: 10141–10144

64 Johnson K N, Hurlock M J, Zhang Q, et al. Balancing noncovalent interactions in the self-assembly of nonplanar aromatic carboxylic acid MOF linkers at the solution/solid interface: HOPG vs. Au(111). Langmuir, 2019, 35: 5271–5280

65 Shi H, Lu X, Liu Y, et al. Nanotribological study of supramolecular template networks induced by hydrogen bonds and van der Waals forces. ACS Nano, 2018, 12: 8781–8790

66 Lei P, Luo W, Tu B, et al. Minor adjustments in the chemical structures of pyridine derivatives induced different co-assemblies by O–H···N hydrogen bonds. Chem Commun, 2022, 58: 9914–9917

67 Li J, Liu B, Duan W, et al. The self-assembly of a low symmetric aromatic carboxylic acid with meta-carboxyl groups regulated by pyridine derivatives. Surf Sci, 2020, 700: 121654

68 Gu J, Wen M, Liang X, et al. Multifunctional aromatic carboxylic acids as versatile building blocks for hydrothermal design of coordination polymers. Crystals, 2018, 8: 83

69 Zhang S, Chen C, Li J, et al. The self-assembly and pyridine regulation of a hydrogen-bonded dimeric building block formed by a low-symmetric aromatic carboxylic acid. Nanoscale, 2022, 14: 2419–2426

70 Jenniches A S, Bahr J, Püschner D, et al. Influence of different substitution patterns on the 2D crystalline aggregation of small molecules on HOPG surfaces. Langmuir, 2022, 38: 6602–6611

71 Zhang X, Chen T, Yan H J, et al. Hydrogen bond partner reorganization in the coadsorption of a monodendron and pyridylethynyl derivatives. Langmuir, 2011, 27: 1292–1297

72 Lackinger M, Griessl S, Markert T, et al. Self-assembly of benzene-dicarboxylic acid isomers at the liquid solid interface: Steric aspects of hydrogen bonding. J Phys Chem B, 2004, 108: 13652–13655

73 Kampschulte L, Griessl S, Heckl W M, et al. Mediated coadsorption at the liquid-solid interface: Stabilization through hydrogen bonds. J Phys Chem B, 2005, 109: 14074–14078

74 Orlando T, Lopes L C, Neumann D A M, et al. Uncovering the origins of supramolecular similarity in a series of benzimidazole structures. CrystEngComm, 2022, 24: 6600–6610

75 Lei P, Ma L, Zhang S, et al. The self-assembly and structural regulation of a hydrogen-bonded dimeric building block formed by two N–H···O hydrogen bonds on HOPG. Chin Chem Lett, 2023, 34: 108005

76 Cristaldi D A, Gulino A. Functionalization of SnO_2 crystals with a covalently-assembled porphyrin monolayer. ChemSusChem, 2013, 6: 1031–

1036
77 Studener F, Müller K, Marets N, et al. From hydrogen bonding to metal coordination and back: Porphyrin-based networks on Ag(111). J Chem Phys, 2015, 142: 101926
78 Ma L, Wang P, Duan W, et al. Regulation of a porphyrin derivative containing two symmetric benzoic acids by different pyridines. Langmuir, 2021, 37: 11544–11551
79 Hou J, Lei P, Meng T, et al. Solvent-dependent self-assemblies and pyridine modulation of a porphyrin molecule at liquid/solid interfaces. Langmuir, 2020, 36: 9810–9817

补充材料

表S1 图1中分子名称缩写全称对应表

本文以上补充材料见网络版csb.scichina.com. 补充材料为作者提供的原始数据, 作者对其学术质量和内容负责.

Summary for “吡啶调控羧酸衍生物组装结构扫描隧道显微镜研究进展”

Progress in scanning tunneling microscopy research on the regulation of carboxylic acids and their derivatives assembled structures by pyridine

Yufei Zhang[1,2], Peng Lei[1,2], Ting Meng[1,2], Chen Wang[1,2*] & Qingdao Zeng[1,2*]

[1] *CAS Key Laboratory of Standardization and Measurement for Nanotechnology, National Center for Nanoscience and Technology (NCNST), Beijing 100190, China;*
[2] *Center of Materials Science and Optoelectronics Engineering, University of Chinese Academy of Sciences, Beijing 100049, China*
* Corresponding authors, E-mail: wangch@nanoctr.cn; zengqd@nanoctr.cn

The supramolecular self-assembly of organic functional molecules on the solid interfaces is a fundamental support for numerous basic and applied research fields. Therefore, the mechanism of self-assembled processes has attracted extensive interest for decades, which provides a theoretical basis for constructing functional nanostructures at the molecular level. Scanning tunneling microscope (STM) can achieve images with a truly atomic scale resolution based on the tunneling current between probes and surfaces. The development of STM opens up a new way to explore the structure and properties of self-assemblies on the two-dimensional (2D) surface. Due to the high-directionality and saturation of hydrogen bonds, the 2D nanostructures driven by intermolecular hydrogen bonding interactions have been widely developed. One of the typical hydrogen bonded networks is formed by carboxylic acid through O–H···O interactions of carboxyl groups between adjacent molecules. However, because of the molecular structure and solvent co-adsorption phenomena at the solid/liquid interface, most of these systems currently studied are homomolecular systems. The reliable preparation method of two-component systems requires the stability of the two-component system exceeds that of any other single-molecular system. The N atom of pyridine is a good acceptor of hydrogen bonds, which has an unpaired electron. Current research shows that carboxyl groups as donors and pyridine as acceptors can preferentially form a binary system based on hydrogen bonds in specific systems. This review summarizes the recent progress in the regulation of carboxylic acids and their derivatives self-assembled structures by pyridine derivatives using STM technology, focusing on how the number and position of functional groups and substituent group of pyridine and carboxylic acid affect the binary systems. Moreover, the self-assembly behavior and co-assembly with pyridine derivatives of rigid, planar and symmetric aromatic carboxylic acids are significantly different from those with low symmetry. The flexible alkyl side chains have structural orientation abilities which can work as molecular templates to accommodate pyridylethynyl derivatives with different sizes and shapes. Fluorination of carboxylic acids can prevent their self-assembly and advantages in the construction of binary networks with different pyridines. Carboxylic acid derivatives containing N heterocycles also show specific co-assembled modes attributed to different strengths of hydrogen bonds donors and acceptors. Carboxyls help porphyrin derivatives form an ordered arrangement through hydrogen bonds and make them can be regulated by different kinds of pyridine. In conclusion, rich binary nanostructures have been constructed which provide effective means for the fabrication and regulation of 2D multicomponent supramolecular assembled structures. However, there are still many shortcomings in this field that require further development. Firstly, we can continue to broaden the basic building blocks of surface nanostructures. For example, we can increase the number of pyridine groups and compare the proportion of O–H···O and O–H···N hydrogen bonds to further deepen the understanding of the co-assembled structure formed by pyridine and carboxylic acids. Secondly, the current understanding of the process and mechanism of surface self-assembly is still insufficient and we are unable to predict the assembled structure accurately. Thirdly, we hope that we can develop more mature surface detection technologies and promote the practical applications of supramolecular self-assembled structures.

molecular self-assembly, carboxylic acid molecules, pyridine regulation, scanning tunneling microscope

doi: 10.1360/TB-2023-0505